Recent experiences with modelling of turbulence chemistry interaction in the context of LES using DNS of turbulent premixed generic planar flame configurations

M. Klein
Fakultät für Luft- und Raumfahrttechnik
Universität der Bundeswehr München, Munich, Germany
Email: markus.klein@unibw.de

Annual meeting of the UK consortium on Turbulent Reacting Flows

Acknowledgements

- <u>Prof. Nilanjan Chakraborty</u>
- <u>Prof. Stewart Cant</u>
- Prof. Hong Im
- Dr. Paul Arias
- Christian Kasten
- Yuan Gao

Outline

- Motivation

- DNS database

- Mathematical background

- LES stresses in turbulent premixed flames

- Scalar fluxes in turbulent premixed flames

- Strategies for turbulent planar flame simulations

- Conclusions & Outlook

Motivation

- Simulation tools are often used to guide the design of energy-efficient & environment-friendly combustion devices.
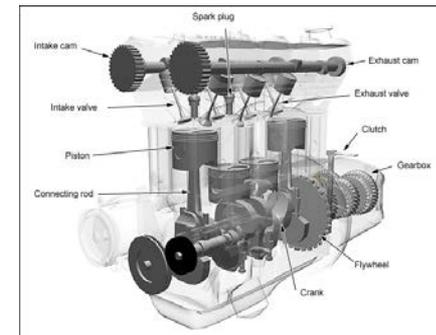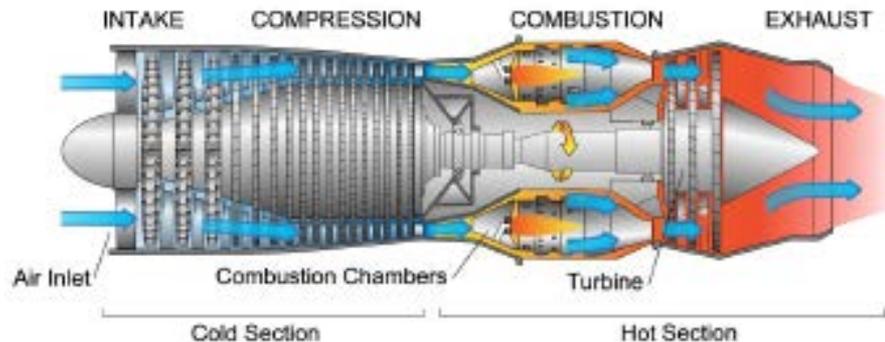
- The system of partial differential equations describing turbulent reacting flows is very complex due to
    - a large range of length and time scales involved and
    - because it involves many degrees of freedom (variables).

- ⇒ A modelling strategy is required in order to be able to deal with the turbulence, the chemical reaction and their mutual interaction.

Large eddy simulation potentially has advantages over traditional methods due to its ability to resolve large-scale turbulent structures.

However, although LES of combustion systems is becoming increasingly popular,

- the closures for sub-grid scale (SGS) stresses have mostly been derived assuming constant density flows
- many closures for the turbulent scalar flux or the chemical source term are generalizations of RANS models

Objectives of this work:

- Better understanding of the physics and the modelling assumptions

- Analysis of existing SGS modelling approaches

- Where possible: improvement of existing SGS models

- Understanding the interaction of numerical and modelling errors

DNS Database

Altogether three databases of turbulent premixed statistically planar flames are considered:

- Two simple chemistry DNS databases

    - They allow a large number of parametric studies in terms of Damköhler number, Karlovitz number, Lewis number, heat release parameter and filter width.
    - Decaying turbulence is considered. Parameters mentioned on the next slides refer to initial values.
    - Principal mechanisms for turbulence chemistry interaction are captured.

- One detailed chemistry database consisting of three H_2/air flames located in three different combustion regimes of combustion.

The first database consists of 5 statistically planar turbulent premixed flames in the thin reaction zones regime <u>with different global Lewis number</u>. In addition case F1 has a reduced <u>heat release parameter</u>.

Cases	Le	u'/S_L	l/δ_{th}	τ	Da	Ka
A1	0.34	7.5	2.45	4.5	0.33	13.0
B1	0.6	7.5	2.45	4.5	0.33	13.0
C1	0.8	7.5	2.45	4.5	0.33	13.0
D1	1.0	7.5	2.45	4.5	0.33	13.0
E1	1.2	7.5	2.45	4.5	0.33	13.0
F1	1.0	7.5	2.45	3.0	0.33	13.0

The turbulent Reynolds number is $Re_t = 47$.
Standard values are chosen for Prandtl (0.7) & Zel'dovich number (6.0).

The second database consists of 5 statistically planar turbulent premixed flames with a range of underlined $Re_t = 22, 23.5, 49, 100, 110$ where the values of Re_t were chosen to vary by changing Ka (Da) while keeping Da (Ka) unaltered.

Cases	u'/S_L	l/δ_{th}	τ	Re_t	Da	Ka
A2	5.0	1.67	4.5	22	0.33	8.67
B2	6.25	1.44	4.5	23.5	0.23	13.0
C2	7.5	2.5	4.5	49.0	0.33	13.0
D2	9.0	4.31	4.5	100.0	0.48	13.0
E2	11.25	3.75	4.5	110	0.33	19.5
F2	15.0	5.72	4.5	216	0.38	24.8

In addition case F2 has a larger scale separation l/δ_{th} and a higher turbulent Reynolds number.

Case	Domain Size	Grid
A1-F1	$24.1\,\delta_{th} \times 24.1\,\delta_{th} \times 24.1\,\delta_{th}$	230×230×230
A2-E2	$36.1\,\delta_{th} \times 24.1\,\delta_{th} \times 24.1\,\delta_{th}$	345×230×230
F2	$32.3\,\delta_{th} \times 32.3\delta_{th} \times 32.3\delta_{th}$	768×768×768
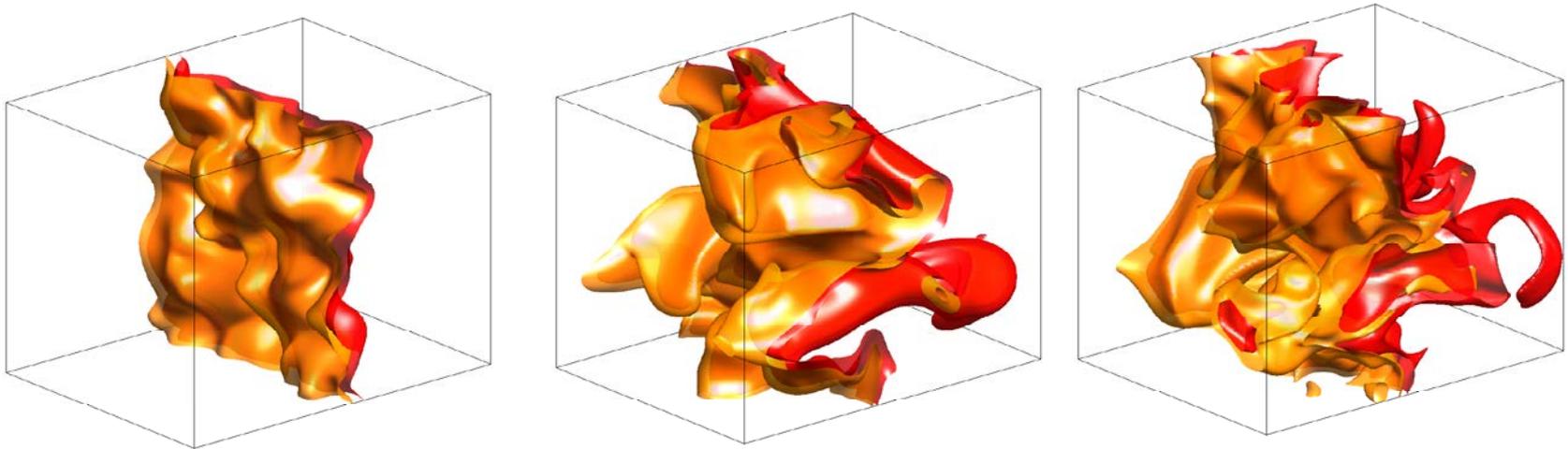
Instantaneous view of c isosurfaces for cases A2, D2 and E2 at $t = \delta_{th}/S_L$. The value of c increases from 0.1 to 0.9 from yellow to red.

- The third database consists of 3 statistically planar turbulent H2-air premixed flames with φ=0.7.

- A detailed chemical mechanism Burke (2012) with 9 species and 19 chemical reactions is employed.

- The flames should be considered as <u>three typical, representative scenarios of the corrugated flamelets, thin reaction zones and broken reaction zones regimes</u> of premixed turbulent combustion, respectively.

Case	u'/S_L	l_T/δ_{th}	Re_t	Da	Ka
A3	0.7	14.0	227	20.0	0.75
B3	5	14.0	1623	2.8	14.4
C3	14	4.0	1298	0.29	126

Case	Domain Size	Grid
A3,B3	$24.1\ \delta_{th} \times 24.1\ \delta_{th} \times 24.1\ \delta_{th}$	512×256×256
C3	$36.1\ \delta_{th} \times 24.1\ \delta_{th} \times 24.1\ \delta_{th}$	1280×320×320
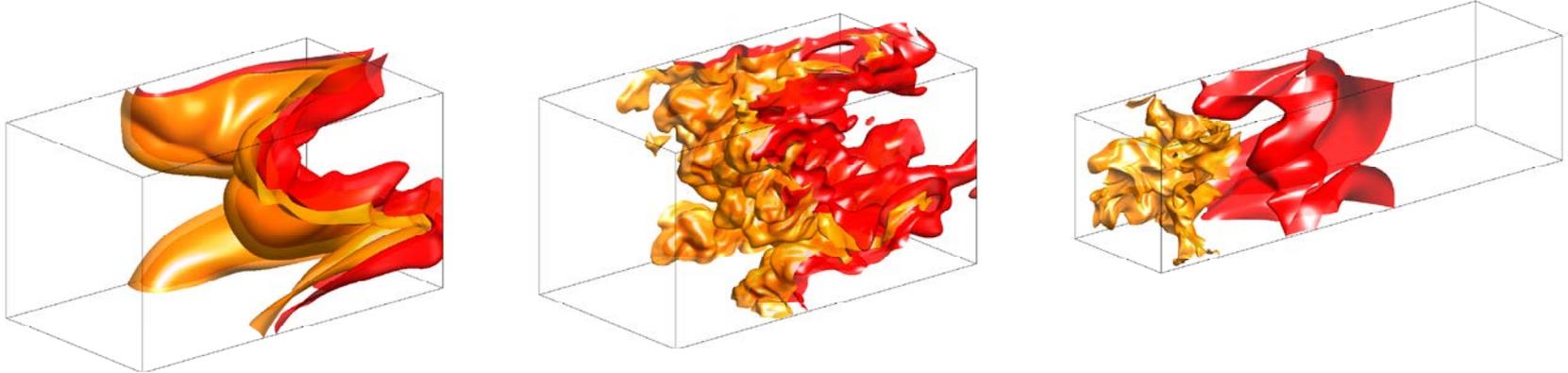
Instantaneous view of c isosurfaces for cases A3, B3 and C3. The value of c increases from 0.1 to 0.9 from yellow to red.

A-priori analysis

- DNS data has been explicitly filtered using a Gaussian filter given by
$$\overline{Q(\boldsymbol{x})} = \int Q(\boldsymbol{x} - \boldsymbol{r})G(\boldsymbol{r})dr \qquad G(\boldsymbol{r}) = (6/\pi\Delta^2)^{3/2}\, exp(-6\, \boldsymbol{r} \cdot \boldsymbol{r}\, /\Delta^2)$$

- For large filter size / computational grid the above filter is for computational economy replaced by the tensor product kernel
$$G(x, y, z) = G(x) \cdot G(y) \cdot G(z) \qquad G(x) = (6/\pi\Delta^2)^{1/2}\, exp(-6\, x^2/\Delta^2)$$

- For constant filter size the computational complexity of the filtering can than be reduced to a linear function of Δ.

- Filtering is performed in parallel using domain decomposition. Each local domain is surrounded by a buffer of the order of the filter width.

- Filter size ranges from $\Delta \approx 0.4\delta_{th}$ up to $\Delta \approx 2.8\delta_{th}$

Numerical Implementation

Simple chemistry	Detailed chemistry
SENGA V1	S3D
3D compressible DNS code	
Single step Arrhenius type chemistry	H_2-air flames, equivalence ratio $\phi = 0.7$ 9 species , 19 reactions
10th order spatial derivatives, dropping to one sided 2nd order	8th order spatial derivatives, dropping to one sided 4th order
Third order low-storage Runge Kutta scheme	Fourth order Runge Kutta scheme
Transverse boundaries are periodic.	
Partially non reflecting NSCBC in direction of mean flame propagation.	Turbulent inflow boundary.

Mathematical background

Under simplifying assumptions the temperature and mass fractions of reactive species can be expressed with a reaction progress variable c.

- This Favre filtered transport equation contains two unclosed terms. Subgrid scalar flux: T^{SGSF} & Filtered flame front displacement: T^{FFFD}

$$\frac{\partial \bar{\rho}\tilde{c}}{\partial t} + \frac{\partial}{\partial x_i}(\bar{\rho}\widetilde{u_i}\tilde{c}) = \underbrace{-\frac{\partial}{\partial x_i}(\overline{\rho u_i c} - \bar{\rho}\widetilde{u_i}\tilde{c})}_{T_i^{SGSF}} + \underbrace{\overline{\frac{\partial}{\partial x_i}\left(\rho D \frac{\partial c}{\partial x_i}\right) + \dot{\omega}_c}}_{T^{FFFD}}$$

Recent research of the author and its collaborators concentrated on these terms individually and in combination:

- T^{FFFD}: PoF, **20**:085108, 2008;
- T^{SGSF}: IJHFF, **52**:28–39, 2015. EJoM B/Fluids, **52**:97-108, 2015.
- $T^{FFFD} + T^{SGSF}$: FTC **96**:921–938, 2016.

Several closures for T^{SGSF} have been analyzed by the authors:

Gradient hypothesis:

$$T_i^{\text{GHM}} = -\frac{\mu_t}{Sc_t}\frac{\partial \tilde{c}}{\partial x_i}, \ \mu_t = (C_s \Delta)^2 \sqrt{2\,\widetilde{S_{ij}}\widetilde{S_{ij}}}, \ \widetilde{S_{ij}} = \frac{1}{2}\left(\frac{\partial \widetilde{u_i}}{\partial x_j} + \frac{\partial \widetilde{u_j}}{\partial x_i}\right)$$

Richard et al. (PROCI, **31**:3059-3066, 2007)

$$T_i^{\text{FRM}} = -\bar{\rho}C_L u_\Delta' \Delta \frac{\partial \tilde{c}}{\partial x_i} - \rho_0 S_L M_i(\bar{c} - \tilde{c}); \ M_i = -\frac{\nabla \tilde{c}}{|\nabla \tilde{c}|} \ u_\Delta' = \sqrt{(\widetilde{u_i u_j} - \tilde{u}_i \tilde{u}_j)/3}$$

Clarks model

$$T_i^{\text{CGM}} = \ \bar{\rho}\frac{\Delta^2}{12}\frac{\partial \widetilde{u_i}}{\partial x_k}\frac{\partial \widetilde{c}}{\partial x_k}$$

Variants of the model T_i^{FRM} with similar physical background did show similar behavior and only one representative will be considered here.

Further, the density weighted momentum conservation equation requires closure of the SGS stress tensor: $\tau_{ij}^{SGS} = \overline{\rho u_i u_j} - \bar{\rho}\widetilde{u}_i\widetilde{u}_j$

$$\frac{\partial \bar{\rho}\widetilde{u}_i}{\partial t} + \frac{\partial}{\partial x_j}\left(\bar{\rho}\widetilde{u}_i\widetilde{u}_j\right) = \frac{\partial}{\partial x_j}\left(\bar{\rho}\,\tilde{v}\left(\frac{\partial \widetilde{u}_j}{\partial x_i} + \frac{\partial \widetilde{u}_i}{\partial x_j}\right) - \frac{2}{3}\bar{\rho}\,\tilde{v}\frac{\partial \widetilde{u_k}}{\partial x_k}\delta_{ij}\right) - \frac{\partial \bar{p}}{\partial x_i}$$

$$\underbrace{-\frac{\partial}{\partial x_j}\left(\overline{\rho u_i u_j} - \bar{\rho}\widetilde{u}_i\widetilde{u}_j\right)}_{\tau_{ij}^{SGS}}$$

Taking the point of view that the isotropic part of the SGS stresses, i.e. the term involving $-\frac{1}{3}\tau_{kk}^{SGS}\delta_{ij}$, can be added to the filtered pressure the static Smagorinsky model takes he following form:

$$\tau_{ij}^{SSM} = -\bar{\rho}v_t 2\left(\widetilde{S_{ij}} - \frac{1}{3}\widetilde{S_{kk}}\delta_{ij}\right) \quad v_t = (C_s\Delta)^2\left|\widetilde{S_{ij}}\right| \quad \widetilde{S_{ij}} = \frac{1}{2}\left(\frac{\partial \widetilde{u}_i}{\partial x_j} + \frac{\partial \widetilde{u}_j}{\partial x_i}\right)$$

The constant C_s is either set to $C_s \approx 0.18$ or can be determined in a dynamic manner (DSM) where $C_d \approx C_s^2$

$$C_d = \frac{M_{ij}\left(L_{ij} - \frac{1}{3}L_{kk}\delta_{ij}\right)}{M_{kl}M_{kl}} \qquad L_{ij} = \bar{\rho}\,\widehat{\widetilde{u_i}\,\widetilde{u_j}} - \frac{\widehat{\bar{\rho}\,\widetilde{u_i}}\,\widehat{\bar{\rho}\,\widetilde{u_j}}}{\widehat{\bar{\rho}}}$$

$$M_{ij} = -2\widehat{\bar{\rho}}\,\widehat{\Delta}^2\left|\widehat{\widetilde{\widetilde{S_{ij}}}}\right|\sqrt{2}\left(\widehat{\widetilde{\widetilde{S_{ij}}}} - \frac{1}{3}\widehat{\widetilde{\widetilde{S_{ij}}}}\delta_{ij}\right) + 2\bar{\rho}\,\Delta^2|\widetilde{S_{ij}}|\sqrt{2}\widehat{\left(\widetilde{S_{ij}} - \frac{1}{3}\widetilde{S_{ij}}\delta_{ij}\right)}$$

The Sigma model (PoF, **23**, (2011), 085106) is a more recent eddy viscosity model used as well for combustion LES:

$$\tau_{ij}^{S\sigma M} = -\bar{\rho}\nu_t 2\left(\widetilde{S_{ij}} - \frac{1}{3}\widetilde{S_{kk}}\delta_{ij}\right) \qquad \nu_t = (C_\sigma\Delta)^2\frac{\sigma_3(\sigma_1 - \sigma_2)(\sigma_2 - \sigma_3)}{\sigma_1^2}$$

$$G_{ij} = \frac{\partial\widetilde{u_j}}{\partial x_i}\frac{\partial\widetilde{u_i}}{\partial x_j} \qquad \sigma_1 \geq \sigma_2 \geq \sigma_3 = \sqrt{\text{Eig}(G_{ij})} \quad C_\sigma = 1.35$$

A variety of scale similarity models has been analyzed:

- Clarks Tensor model reads: $\tau_{ij}^{CTM} = \bar{\rho}\,\dfrac{\Delta^2}{12}\,\dfrac{\partial \widetilde{u_i}}{\partial x_k}\,\dfrac{\partial \widetilde{u_j}}{\partial x_k}$

- Velocity based scale similarity: $\tau_{ij}^{VSS} = \bar{\rho}\left(\overline{\widetilde{u_i}\widetilde{u_j}} - \overline{\widetilde{u_i}}\,\overline{\widetilde{u_j}}\right)$

- Density based scale similarity: $\tau_{ij}^{DSS} = \overline{\bar{\rho}\widetilde{u_i}\widetilde{u_j}} - \overline{\bar{\rho}\widetilde{u_i}}\,\overline{\bar{\rho}\widetilde{u_j}}/\bar{\bar{\rho}}$

- Interscale energy transfer: $\tau_{ij}^{IET} = \bar{\rho}\left(\widehat{\widehat{\widetilde{u_i}}\widetilde{u_j}} + \widehat{\widetilde{u_i}\widehat{\widetilde{u_j}}} - \widehat{\widetilde{u_i}}\widehat{\widetilde{u_j}} - \widehat{\widehat{\widetilde{u_i}}\widehat{\widetilde{u_j}}}\right)$

The IET model is an adaption of a recent proposal by Domaradzki (PoF, **24**, (2012), 065104) with potentially better energy transfer properties to compressible flows.

Note that the IET model requires two test filter levels.

An alternative to adding the isotropic part of the SGS tensor to the filtered pressure is the model suggested by Yoshizawa:

$$\tau_{kk}^{SGS} = 2\, C_I \bar{\rho}\, \Delta^2 \left| \widetilde{S_{ij}} \right|^2$$

If the isotropic part τ_{kk} is explicitly modelled the combined model is denoted as the SSY model in this paper.

Yoshizawa recommended $C_I = 0.089$, whereas Moin reported values in the range $0.0025 - 0.009$.

All past studies regarding the SSY model have been performed in the context of non-reacting flows.

Results – Modelling of τ_{ij}^{SGS}

Case A2

$\Delta=0.4\delta_{th}$
$\Delta=1.2\delta_{th}$
$\Delta=2.0\delta_{th}$
$\Delta=2.8\delta_{th}$

Case C2

Δ increases

Ka increases

Case E2
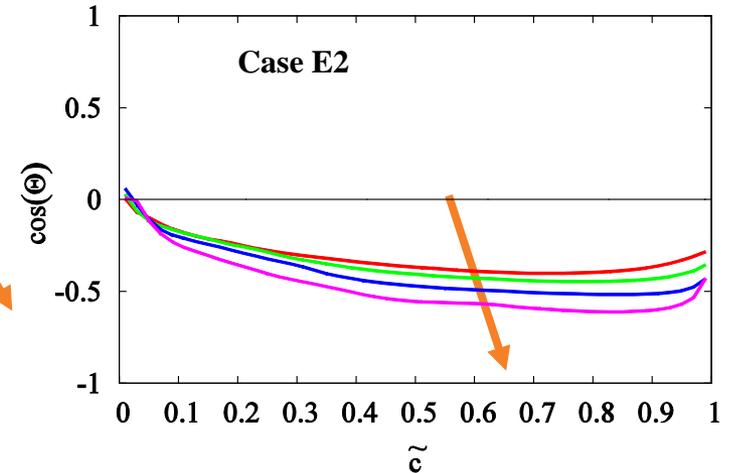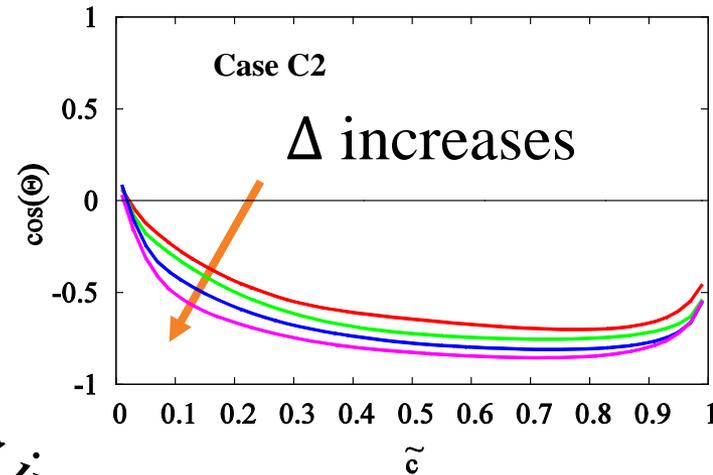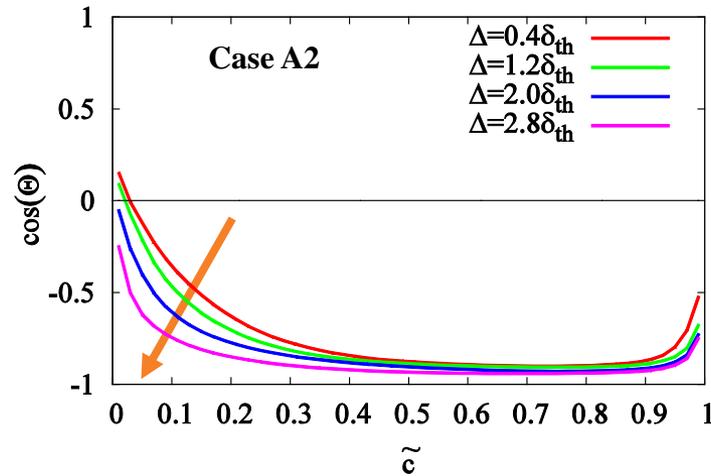
Cosine of the angle Θ between τ_{1j}^{SGS} calculated from DNS and τ_{1j}^{SSM} predictions conditional on $\tilde{c}$ for cases A2 ($Ka = 8.65$), C2 ($Ka = 13.0$) and E2 ($Ka = 19.5$), for four different filter widths.

Case A2

Case C2

Case E2
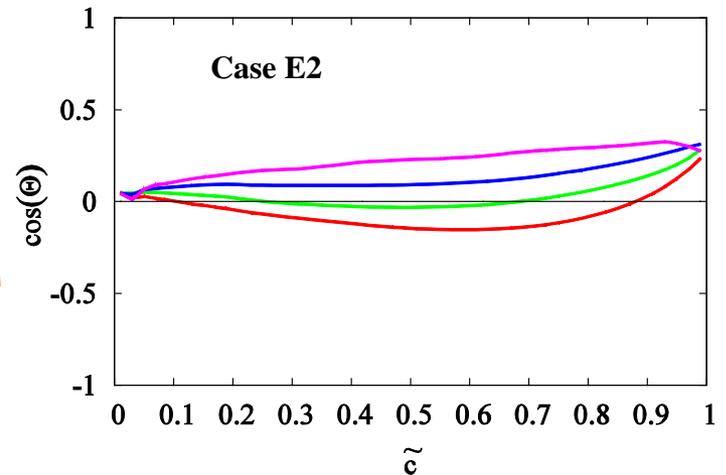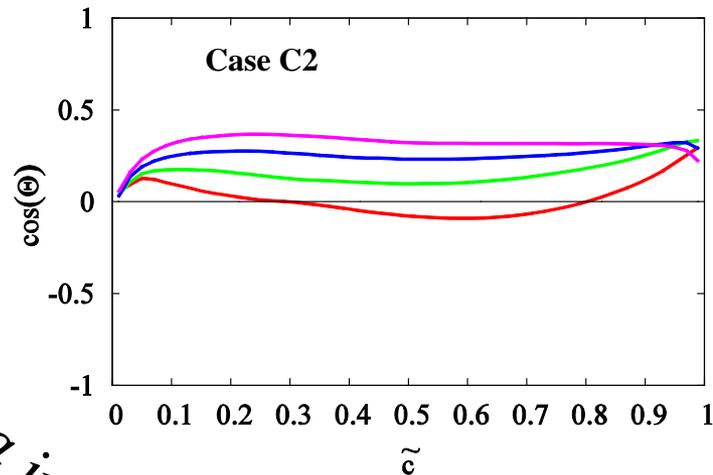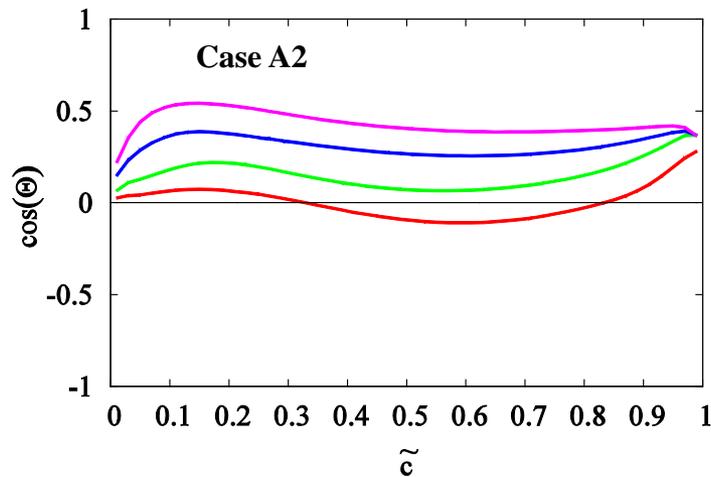
Ka increases

Cosine of the angle Θ between τ_{2j}^{SGS} calculated from DNS and τ_{2j}^{SSM} predictions conditional on $\widetilde{c}$ for cases A ($Ka = 8.65$), C ($Ka = 13.0$) and E ($Ka = 19.5$), for four different filter widths.

Discussion

- A negative Θ indicates opposite (counter-gradient - CGT) alignment between modelled SGS stress and SGS stress from DNS

- CGT increases for the component τ_{11} in flame propagation direction with increasing u'/S_L and with increasing filter width

- Similarly (not shown), CGT increases with decreasing heat release parameter or Lewis number (due to thermo-diffusive instability)

- This behavior is in analogy to the turbulent scalar flux where it is known that the amount of CGT depends on the competition between turbulent velocity fluctuation and heat release
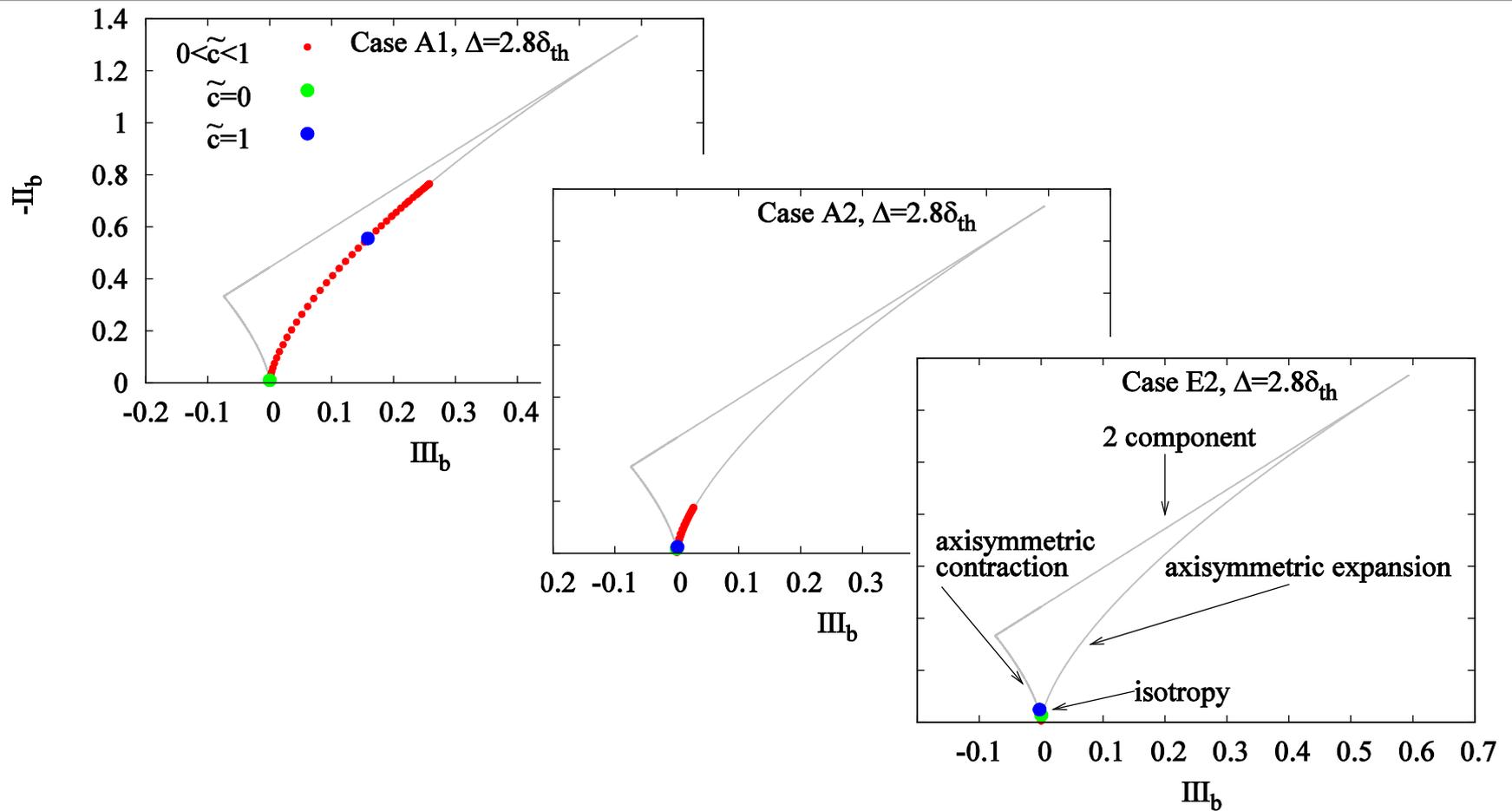
τ_{ij}^{SGS} based Lumley triangle for A1,A2,E2, $\Delta = 2.8\delta_{th}$.

Red dot represents an average conditional on $\tilde{c}$. Points for $\tilde{c} = 0,1$ are shown in green respectively blue.

Discussion

- Cases A1 where $Le \ll 1$ and A2 where u'/S_L is relatively small show the strong effects of anisotropy arising from high values of dilatation.

- This axisymmetric expansion represents the flow state of a planar flame where mean direction of propagation is aligned with x_1 axes.

- Simulations are started from an initially isotropic turbulent flow field. Only for case A1 the anisotropy remains on the burned gas side.

- The relatively poor performance of eddy viscosity models can be explained by looking at the Lumley triangle.

- The strength of CGT for the stress components is linked to the strong axisymmetric expansion.

A remark regarding the dynamic model:
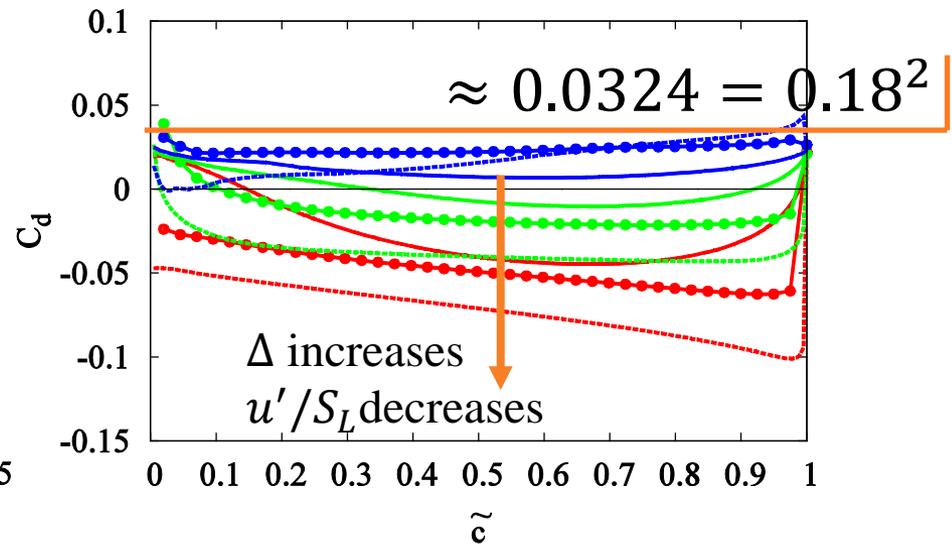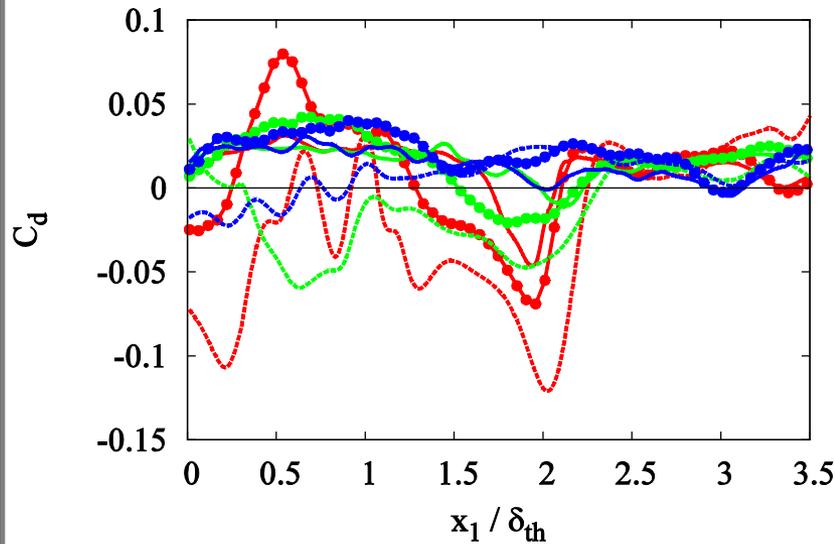
Variation of the dynamic Smagorinsky parameter C_d versus x_1 resp. $\tilde{c}$.
LHS: C_d is determined after spatial averaging of numerator and denominator of the C_d expression;
RHS: Averages are calculated conditional on $\tilde{c}$.

Case A2, $\Delta=0.4\delta_{th}$ ———
Case A2, $\Delta=1.6\delta_{th}$ ——●——
Case A2, $\Delta=2.8\delta_{th}$ - - - -
Case D2, $\Delta=0.4\delta_{th}$ ———
Case D2, $\Delta=1.6\delta_{th}$ ——●——
Case D2, $\Delta=2.8\delta_{th}$ - - - -
Case E2, $\Delta=0.4\delta_{th}$ ———
Case E2, $\Delta=1.6\delta_{th}$ ——●——
Case E2, $\Delta=2.8\delta_{th}$ - - - -

Discussion

- A standard averaging procedure for determining the model parameter C_d yields rather unsatisfactory results in this context.

- As a result it can happen, that the DSM model performs even worse (not shown here) than its static counterpart.

- The figure on the RHS demonstrates clearly that the Smagorinsky parameter should be a function of $\tilde{c}$.

- In the middle of the flame brush, C_d becomes small or even assumes negative values, which is in agreement with the CGT observation.

Comparison of the Sigma model and the Smagorinsky model
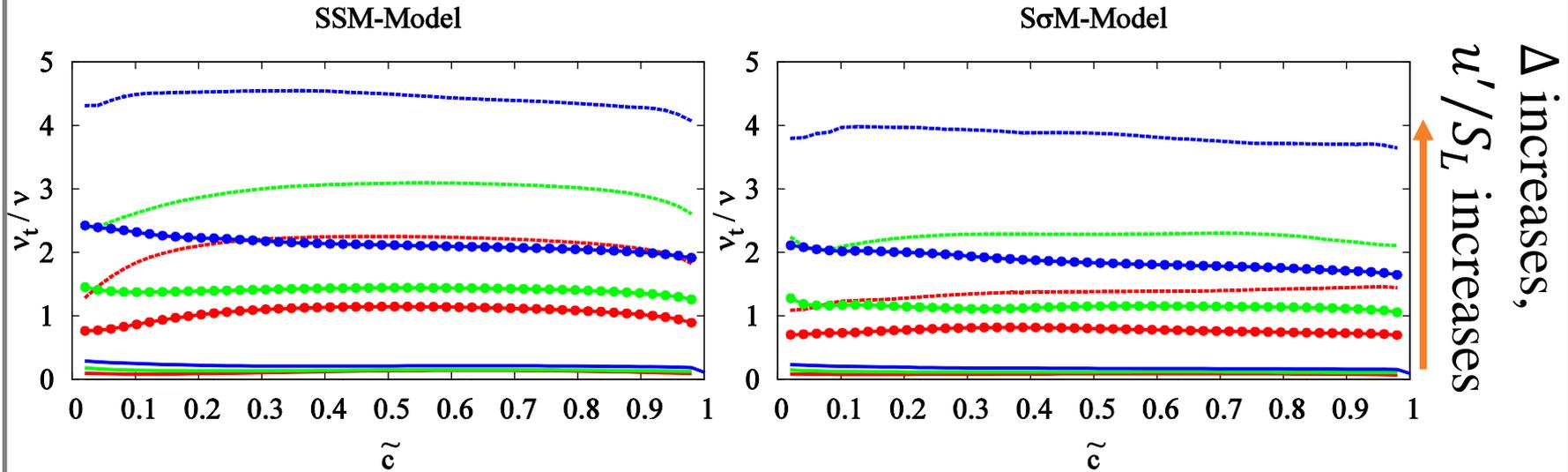
Comparison of the mean values of normalised turbulent viscosities obtained from the SSM and the sigma Model SσM conditional on $\tilde{c}$.

Discussion

- Mean turbulent viscosities predicted by the SσM model are somewhat smaller than those predicted by the SSM model, but this is a matter of tuning the constants C_s and C_σ.

- The mean behavior for these two models is very similar.

- The SσM model has higher fluctuations which is not shown.

- Although the SσM model does not provide advantages within the flame brush this might be the case close to walls.

Can things be improved if the isotropic part is modelled and what is a suitable value of C_I ?

$$\tau_{ij}^{SSM} = -\bar{\rho}\nu_t 2\left(\widetilde{S_{ij}} - \frac{1}{3}\widetilde{S_{kk}}\delta_{ij}\right) + \frac{1}{3}2C_I\bar{\rho}\,\Delta^2\left|\widetilde{S_{ij}}\right|^2\delta_{ij}$$
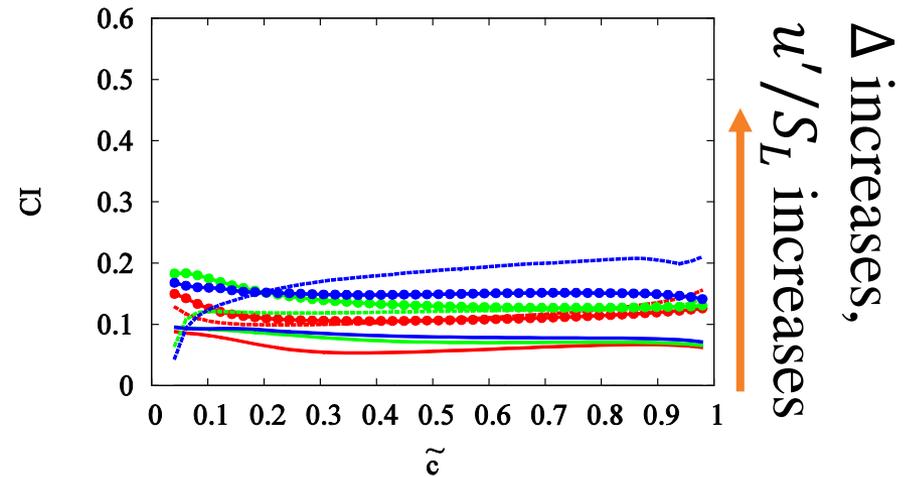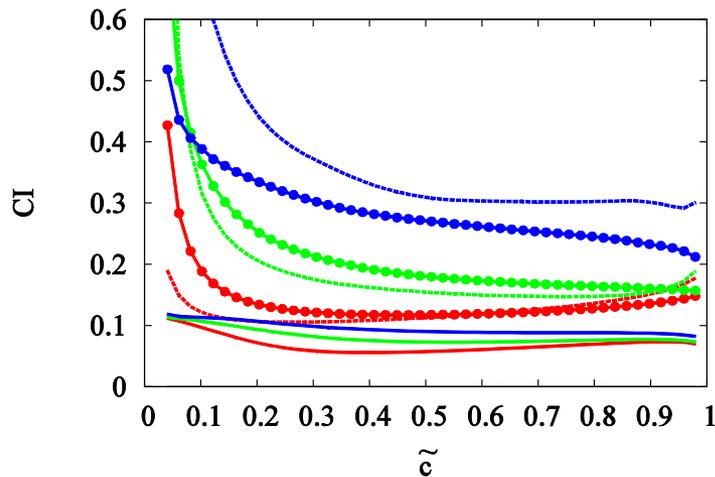
Dynamic evaluation of the model parameter CI.
LHS: CI is determined after conditional averaging of numerator and denominator in $C_I = \langle L_{kk}\rangle / \langle M\rangle$ following Moin et al.
RHS: Averages are calculated according to $C_I = \langle L_{kk}M\rangle / \langle M^2\rangle$

Discussion:

- If at all dynamic determination of C_I works only if conditional averaging is applied.

- The formula $C_I = \langle L_{kk} M \rangle / \langle M^2 \rangle$ works better than $C_I = \langle L_{kk} \rangle / \langle M \rangle$

- Values of C_I are considerably larger than those reported in the literature for non-reacting flows.

Correlation analysis

τ_{kk}^{SGS} modelled   Scale Similarity Type Models
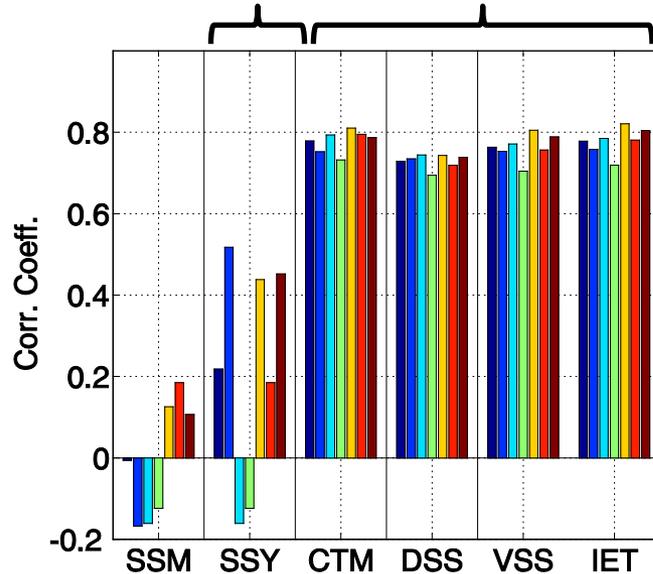
$$0.1 \leq \bar{c} \leq 0.9$$
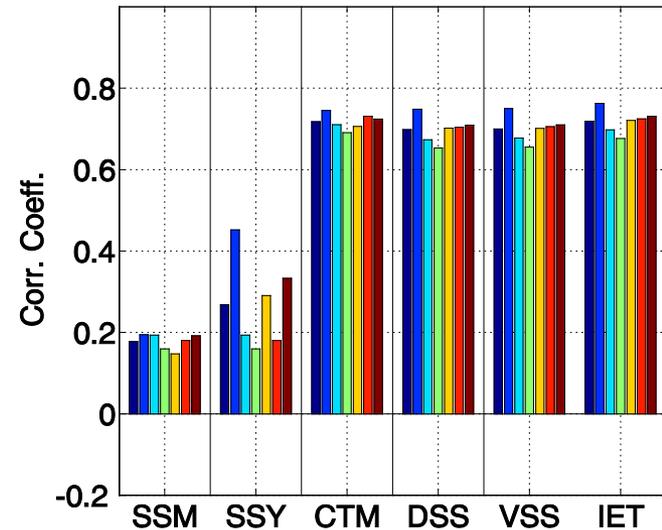
$$0.0 \leq \bar{c} \leq 0.1$$

Correlation coefficients (averaged over all filter width and cases) for the models SSM, SSY, CTM, DSS, VSS, IET: τ_{mean}^{SGS} (■); τ_{11}^{SGS} (■); τ_{12}^{SGS} (■); τ_{13}^{SGS} (■); τ_{22}^{SGS} (■); τ_{23}^{SGS} (■); τ_{33}^{SGS} (■).

Discussion

- SSM model correlates negatively for all components involving contributions in the direction of mean flame propagation (i.e. τ_{1j}^{SGS}).

- Correlation coefficients of the stress components $\tau_{11}^{SGS}(!), \tau_{22}^{SGS}, \tau_{33}^{SGS}$ increase considerably when the isotropic part is modelled (SSY).

- Scale similarity type models show considerably higher correlations. Highest overall correlation is obtained for the CTM and IET model.

- The correlation coefficients towards the unburned gas side are representative for non-reacting flows.

- This shows again that the negative correlation is essentially due to dilatation effects.

The correlation analysis is invariant under multiplication of the model with a scalar.
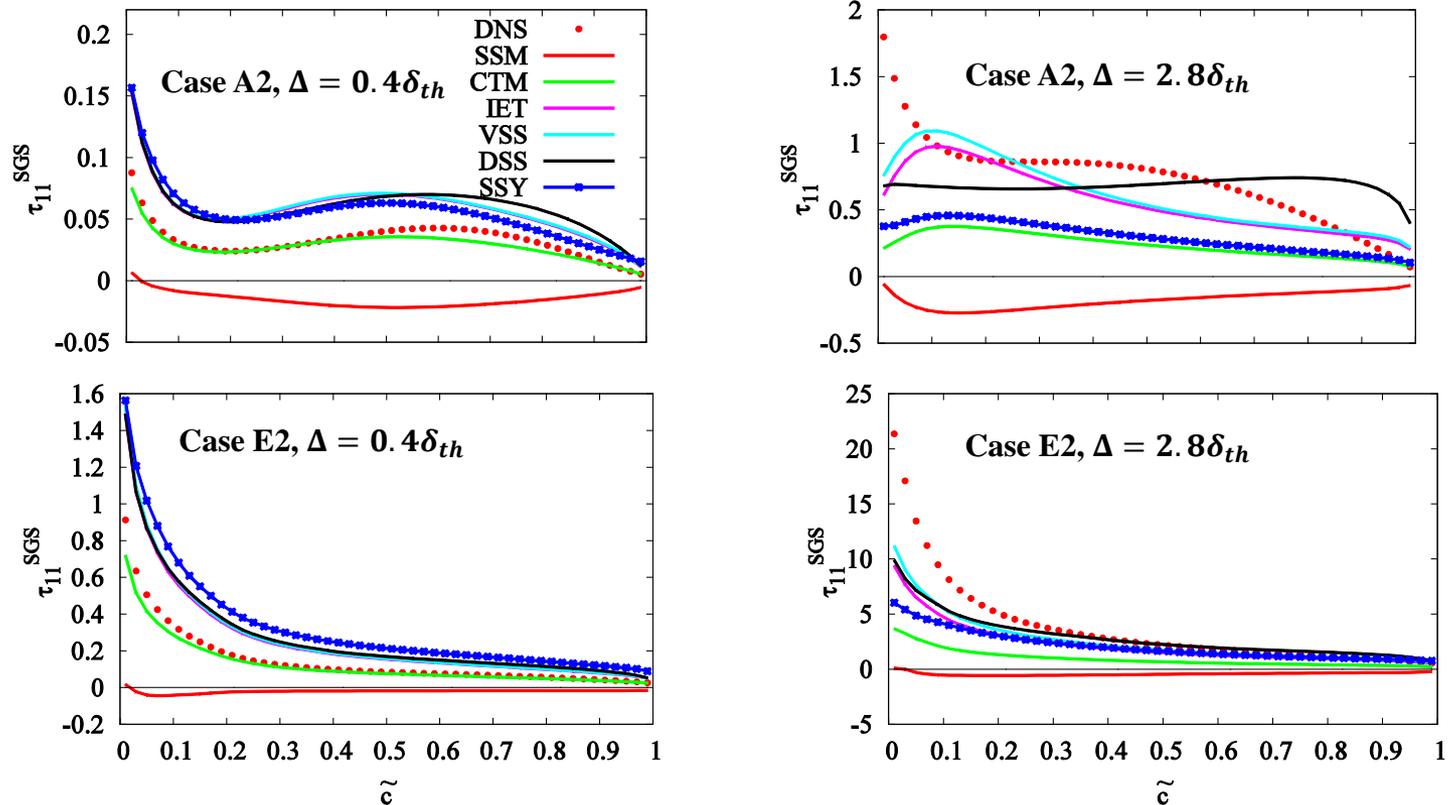
Conditional plot of τ_{11}^{SGS} from DNS as well as different model expressions against $\tilde{c}$ for filter width $\Delta \approx 0.4\delta_{th}, \Delta \approx 2.8\delta_{th}$ for cases A2 (left) and E2 (right).

Discussion

- Eddy viscosity models depict the wrong sign of the (flame normal) stress component.

- Modelling of the isotropic part of the stress tensor improves the results for eddy viscosity models.

- Scale similarity models predict the stresses reasonably for small filter size but tend to under-predict the magnitude for large filter size.

- There is no single model that is able to provide satisfactory results for all cases and all filter width.

Modelling the trace of the stress tensor is not only useful for closing the momentum equation.

- The generalised SGS kinetic energy is frequently used for estimating which portion of the TKE is resolved (<u>quality assessment</u>).

- Furthermore τ_{kk}^{sgs} is often required as a <u>submodel for closing the chemical source term</u>.

- Therefore it is useful to have a closer look to the modelling of τ_{kk}^{sgs}.

- The Lewis number database is considered for this purpose.

- Besides the YOS model the trace of any scale similarity model can be used for modelling τ_{kk}^{sgs} (CTM and DSS are considered here)

- Comparing YOS $2\,C_I\bar{\rho}\,\Delta^2\left|\widetilde{S_{ij}}\right|^2$ with CTM $\bar{\rho}\dfrac{\Delta^2}{12}\dfrac{\partial\widetilde{u_i}}{\partial x_k}\dfrac{\partial\widetilde{u_i}}{\partial x_k}$ shows that 9 out of 12 terms contained in the YOS model are identically the same.

- This provides an opportunity to come up with an estimated model coefficient of $C_I = (1/48) - (1/24)$ on a entirely different route.

- $C_I = (1/24)$ will be used in the following.

- The trace of the CTM model can furthermore be analytically reformulated as: $\tau_{kk}^{CTM*} = \bar{\rho}\,(\Delta^2/24)\left(\partial^2\widetilde{u_k}^2/\partial x_i^2 - 2\widetilde{u_k}\,\partial^2\widetilde{u_k}/\partial x_i^2\right)$.

- A-priori filtered DNS data is available on the DNS grid.

- Evaluating LES models on the DNS respectively LES grid, gives an indication regarding the model formulation and how much it is affected by numerical errors/differentiation.
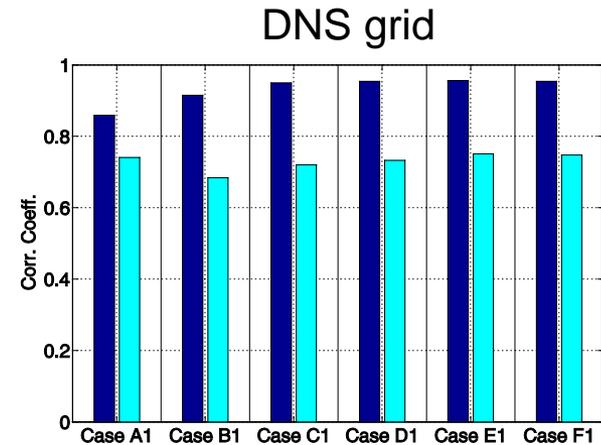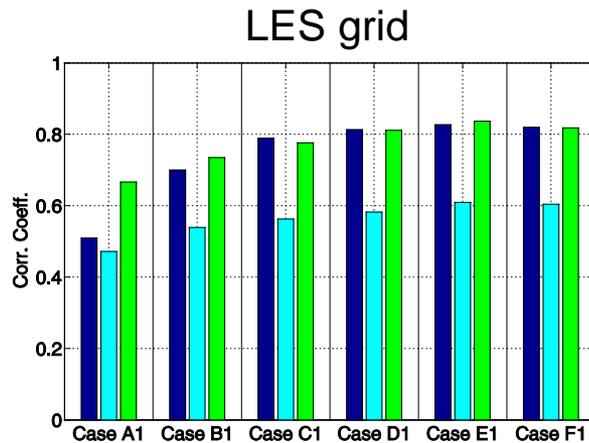
LES grid — DNS grid

Correlation coefficients between modelled and the corresponding value extracted from DNS: CTM (■); YOS (■); DSS (■);

LHS: Gradients are evaluated on the LES grid.

RHS: Gradients are evaluated on the DNS grid.

Correlations are lower on the DNS grid. This is due differentiation errors as well as a decreasing accuracy of the Taylor approximation.

The magnitude of the model can be adjusted via the model multiplier.
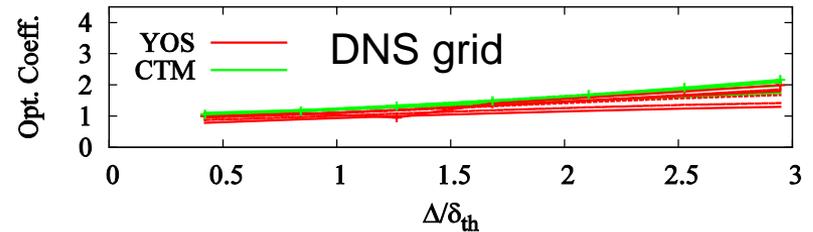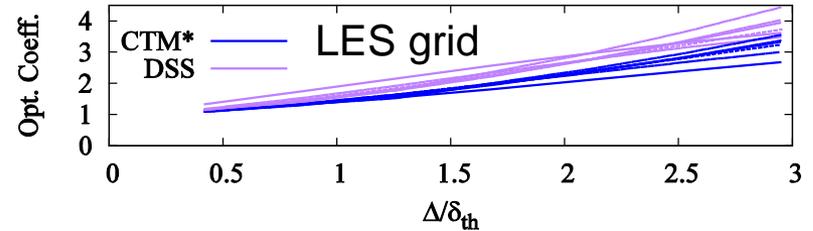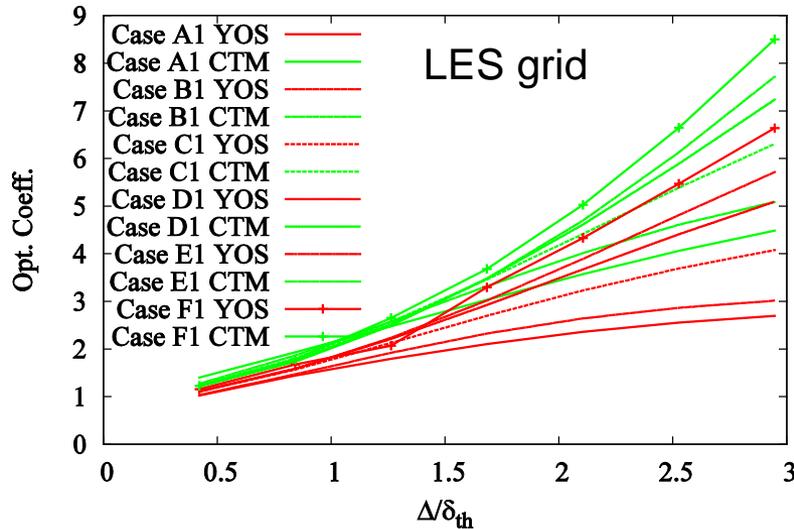
Variation of <u>optimum model multipliers </u>with Δ.

LHS: YOS and CTM model. Gradients are evaluated on the LES grid.

RHS-TOP: DSS model and CTM* model where gradients are evaluated on the LES grid.

RHS-BOTTOM: YOS and CTM model. Gradients are evaluated on the DNS grid.

Discussion

- The optimal model coefficient converges towards unity if $\Delta \to \Delta_{\text{DNS}}$, which is consistent with the theoretical derivation of the CTM model.

- $C_I = 1/24$ for the YOS model, is reasonable (for small Δ).

- Optimal model coefficients increase consistently with increasing Δ, and this behaviour is more pronounced going from case A1 to F1.

- The CTM* model is superior to the CTM model. This can be explained based on the modified wavenumber analysis.

- CTM & YOS model considerably under-predict GSGS TKE for large filter width. They should not be used for LES quality assessment !!

- Complex interaction between numerical and physical modelling !

Reviewer concerns

This is not based on modern combustion DNS:

- The database has limited range of scales

- The database has too low turbulent Reynolds number

- The simple chemistry assumption will affect the results

- The decaying turbulence configuration is unphysical

- Decaying turbulence does not provide enough samples

I will in the following address several of the reviewers concerns and show that the qualitative behavior of our results does not change

- If the turbulent Reynolds number is considerably higher.

- If detailed chemistry is uses instead of simple chemistry.

- If the flow configuration is changed.

This doesn't mean that these concerns are irrelevant in general.

But they do not apply to physical mechanisms (in terms of turbulence chemistry) interaction we were looking at.

Range of Scales

Cases	u'/S_L	l/δ_{th}	τ	Re_t	Da	Ka
F2	15.0	5.72	4.5	216	0.38	24.8

Case	Domain Size	Grid
F2	$32.3\,\delta_{th} \times 32.3\delta_{th} \times 32.3\delta_{th}$	768×768×768
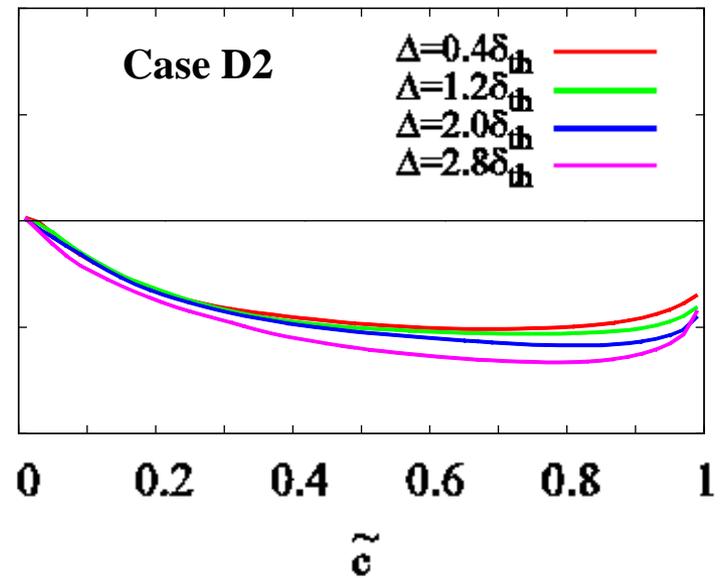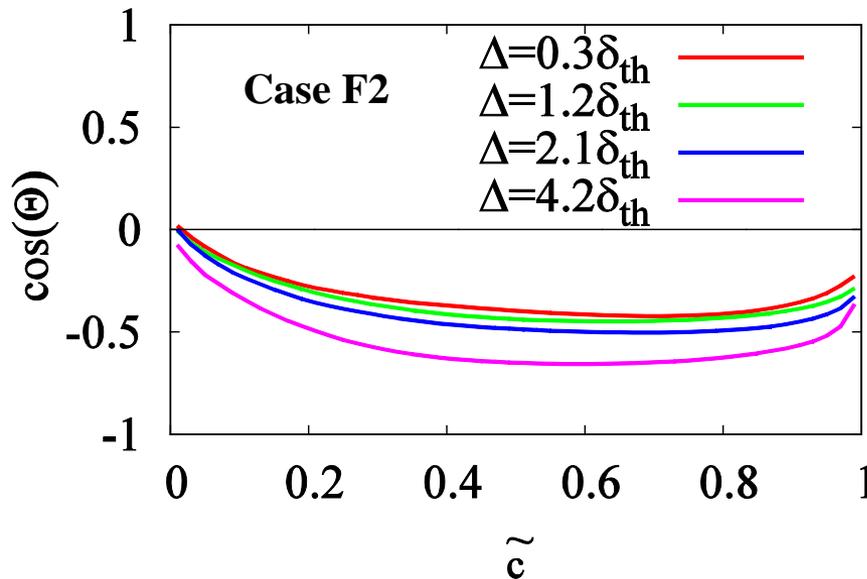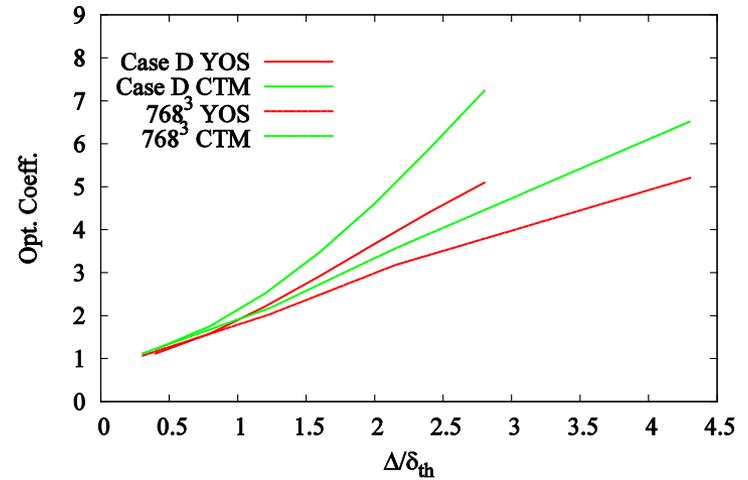
Detailed Chemistry

- Instead of showing the simple chemistry results for scalar flux modelling the attention will be directly focused on detailed chemistry.

- It is however noted that the simple chemistry analysis is much more detailed.

- Another important difference of this database is the flow configuration. A turbulent inflow is used here.

- Instead of $\bar{\rho}(\widetilde{u_i c_T} - \widetilde{u_i}\widetilde{c_T})$ the focus is now on $\bar{\rho}(\widetilde{u_i Y_m} - \widetilde{u_i}\widetilde{Y_m})$

- Obviously gradient flux has the opposite sign for a reactant and a product species. What about CGT ?

- For reaction progress variable c_T it can be shown (Bray *et al.*,1981) that in the limit of thin flames the turbulent scalar flux takes the form: $\tau_{i,c} \approx \bar{\rho}\tilde{c}(1-\tilde{c})[\overline{(u_i)_P} - \overline{(u_i)_R}]$ $\overline{(u_i)_{P/R}}$: conditionally filtered velocity

- This can lead to $\overline{(u_i)_P} > \overline{(u_i)_R}$ and hence $\tau_{i,m} > 0$ for product mass fractions in contradiction with the gradient hypothesis closure.

- For a reaction regress variable b (which decreases monotonically from 1 in the fresh gas to 0 in the fully burned products) the flux can be expressed as $\tau_{i,b} \approx \bar{\rho}\tilde{b}(1-\tilde{b})[\overline{(u_i)_R} - \overline{(u_i)_P}]$

- Hence, by analogy, $\tau_{i,b} < 0$ for reactant species, again in contra-diction with the gradient hypothesis closure.
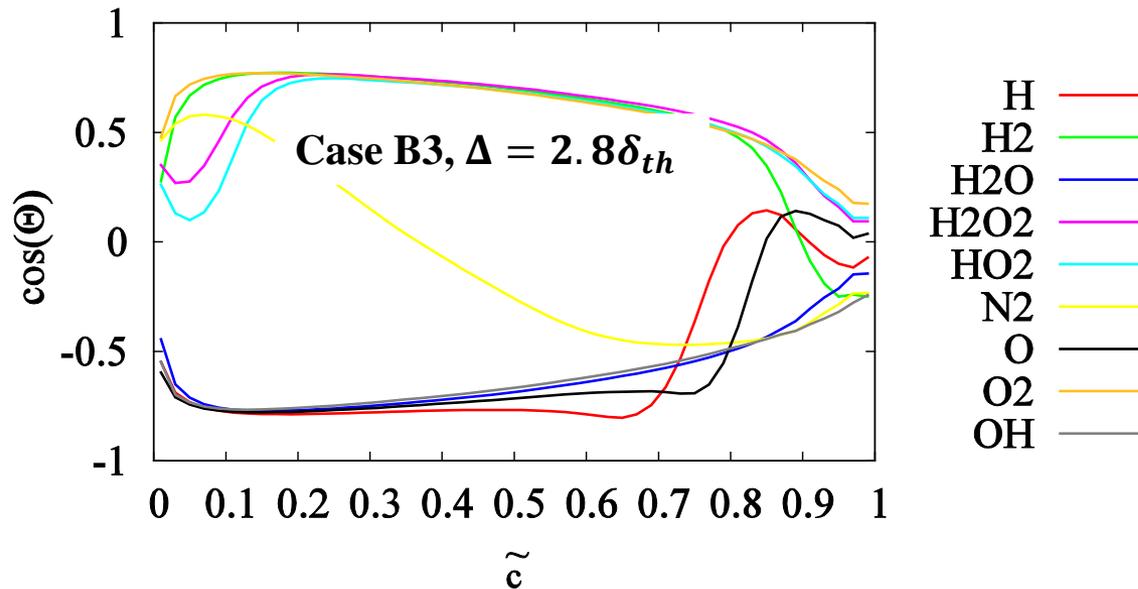
Cosine of the angle Θ between $\bar{\rho}\left(\widetilde{u_i\,Y_m} - \widetilde{u_i}\widetilde{Y_m}\right)$ for different species m calculated from DNS and $-\partial\widetilde{c_T}/\partial x_i$ predictions conditional on $\widetilde{c}$ for case B and filter width $\Delta \approx 2.8\delta_{th}$.

The opposite alignment of species H, O, OH, H_2O and H_2, O_2, HO_2, H_2O_2 can be clearly seen.

This has modelling implications for the FRM model.
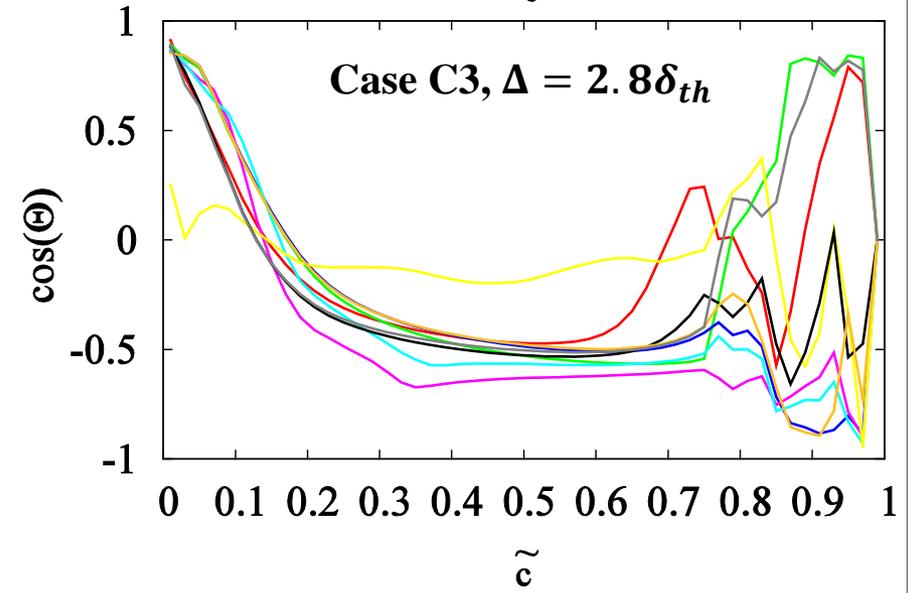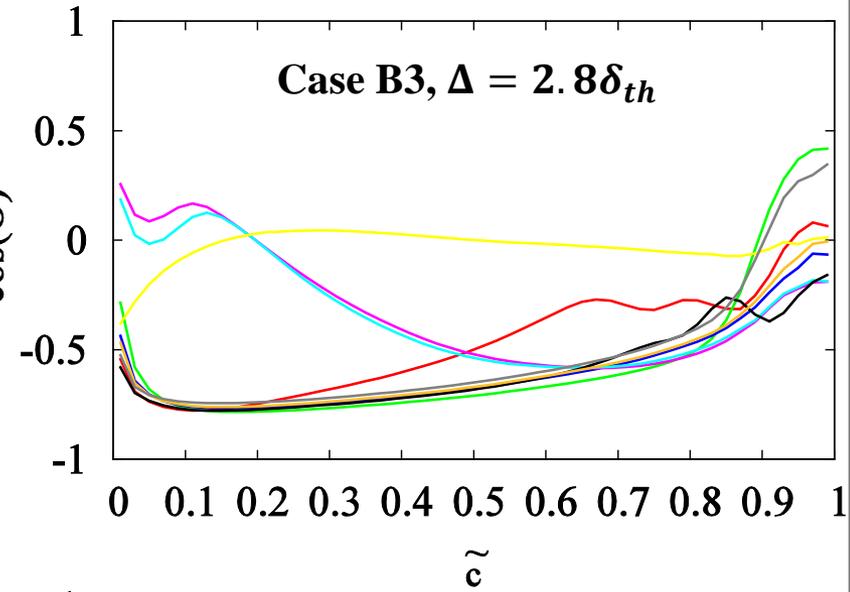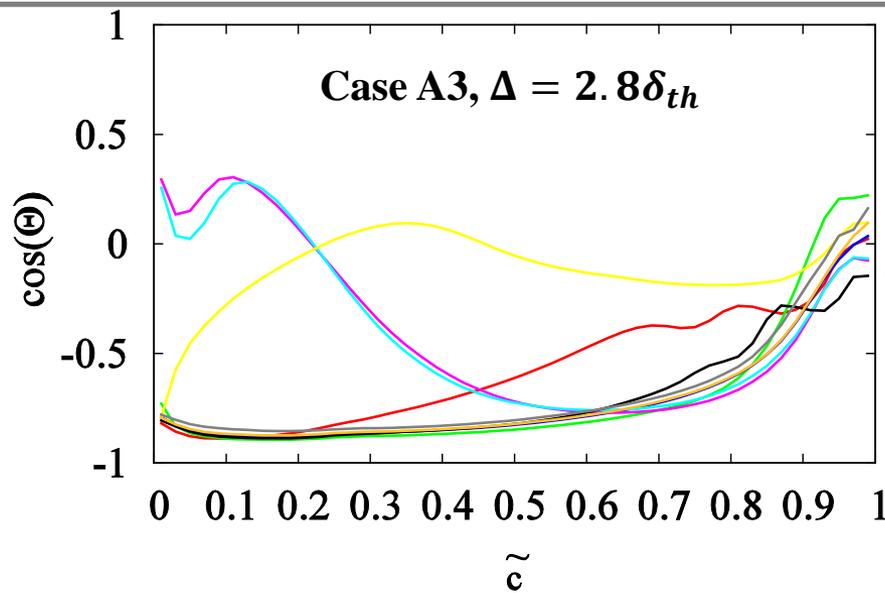
Case A3, $\Delta = 2.8\delta_{th}$

Case B3, $\Delta = 2.8\delta_{th}$

Case C3, $\Delta = 2.8\delta_{th}$

Ka increases

Cosine of the angle Θ between $\bar{\rho}\left(\widetilde{u_i\,Y_m} - \widetilde{u_i}\widetilde{Y_m}\right)$ for different species m calculated from DNS and $-\partial\widetilde{Y_m}/\partial x_i$ predictions conditional on $\widetilde{c}$ for cases A3, B3, C3 for filter width $\Delta \approx 2.8\delta_{th}$.

Negative of correlation is shown for GHM

Case B3

Case C3
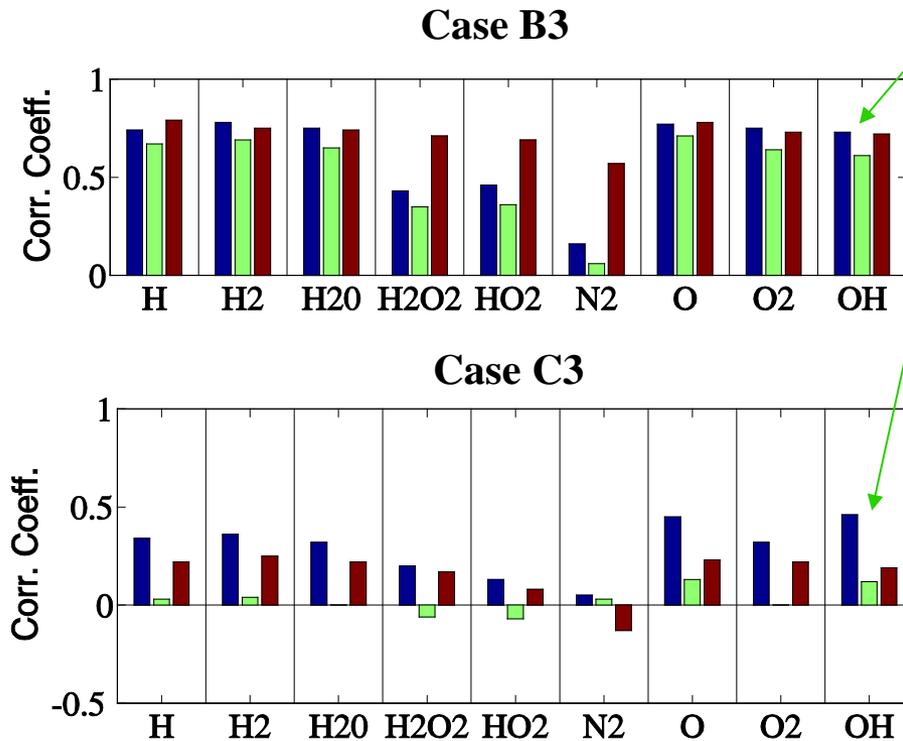
$$T_i^{\text{FR}M} =$$
$$-\bar{\rho} C_L u'_\Delta \Delta \frac{\partial \tilde{c}}{\partial x_i}$$
$$-\rho_0 S_L M_i \left(\overline{Y_m} - \widetilde{Y_m} \right);$$
$$M_i = -\frac{\nabla \tilde{c}}{|\nabla \tilde{c}|}$$

Correlation coefficients between modelled and actual values of
$\bar{\rho}\left(\widetilde{u_i\, Y_m} - \widetilde{u_i}\, \widetilde{Y_m} \right)$ in the range $0.1 \leq \bar{c} \leq 0.9$.
Models $\tau_{i,m}^{CGM}$ (■), $\tau_{i,m}^{GHM}$ (■) and $\tau_{i,m}^{FRM}$ (■) for cases B3,C3, $\Delta \approx 2.8 \delta_{th}$.
The negative of the correlation coefficient is shown for the GHM model.

Detailed Chemistry / Inflow

Case B3, $\Delta = 2.8\delta_{th}$

Different species

Simple Chemistry / Decaying

Case A2, $\Delta = 2.8\delta_{th}$

Negative of correlation is shown for GHM

Corr. Coeff.

H   H2   H20   H2O2   HO2   N2   O   O2   OH   c
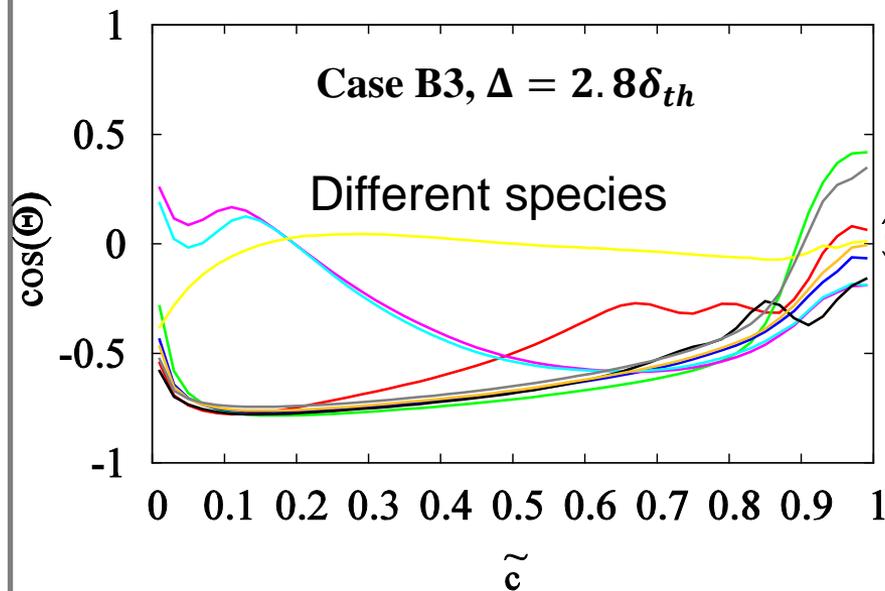
Detailed Chemistry / Inflow   Simple Chemistry / Decaying

$\tau_{i,m}^{CGM}$ (■)

$\tau_{i,m}^{GHM}$ (■)

$\tau_{i,m}^{FRM}$ (■)

Case B3, $\Delta = 2.8\delta_{th}$

Case C3, $\Delta = 2.8\delta_{th}$
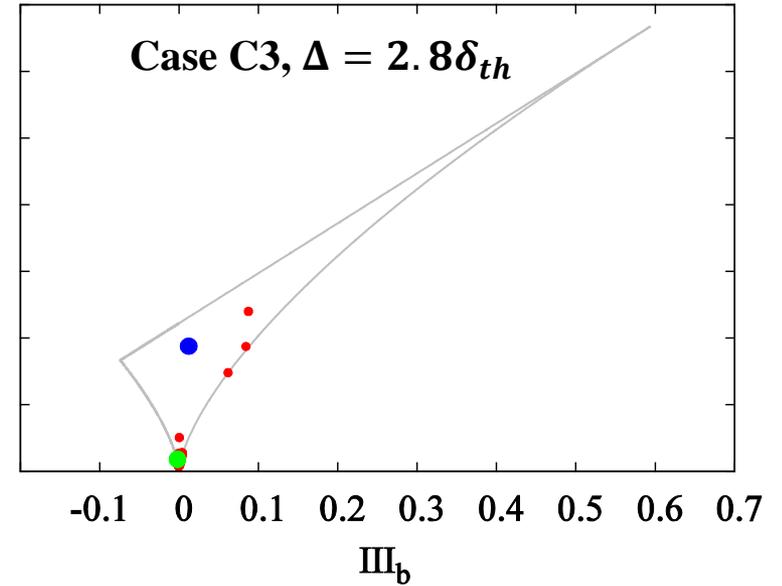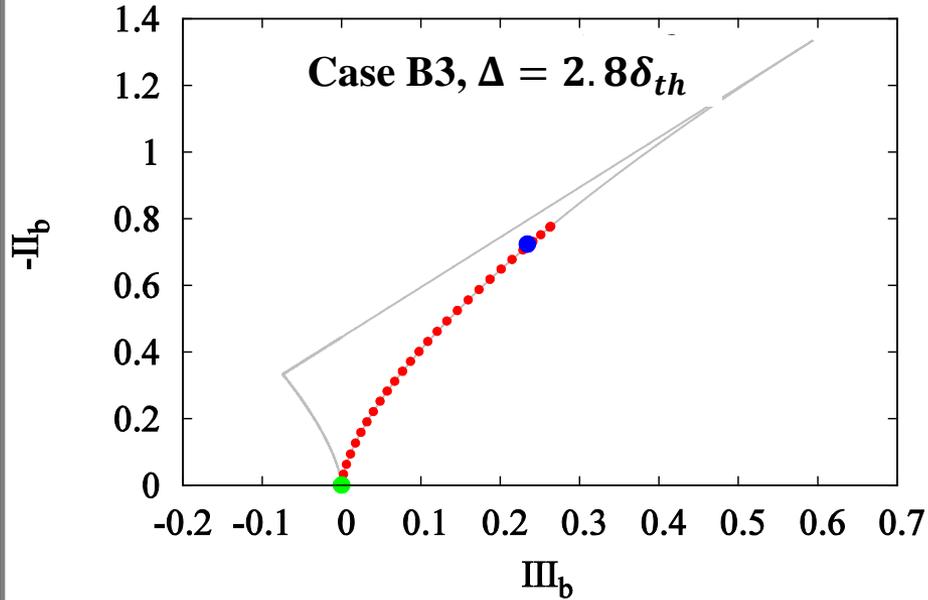
LES based Lumley triangle for B3,C3,$\Delta = 2.8\delta_{th}$. A3 looks similar to B3. Red dot represents an average conditional on $\tilde{c}$. Points for $\tilde{c} = 0,1$ are shown in green respectively blue.

Strategies for planar flame simulations

- Statistically planar turbulent premixed flames are an important canonical flow configuration

- They have zero mean flame curvature and statistical analysis is simplified because flow quantities vary only in flame normal direction

- There exist essentially three different methods to introduce the turbulence in the computational domain

Three methods will be compared and analysed on the next slides

- Decaying turbulence (DT):
  The flow field is initialised with divergence free velocity fluctuations.
  Turbulence decays with time and statistics are recorded after a few
  eddy turnover times.

- Inflow / outflow configuration (IO):
  A turbulent inflow condition maintains the desired turbulence level.
  Statistics are extracted after reaching a steady state.
  Mean inflow velocity needs to be adjusted.

- In the Lundgren forcing (LF):
  A linear volume forcing term $f = (\varepsilon/2k)\, u$ as suggested by Lundgren
  (2003) is used to maintain turbulence.
  Another volume forcing implementation uses a long-wavelength density
  weighted forcing but will not be considered here.

Decaying Turbulence
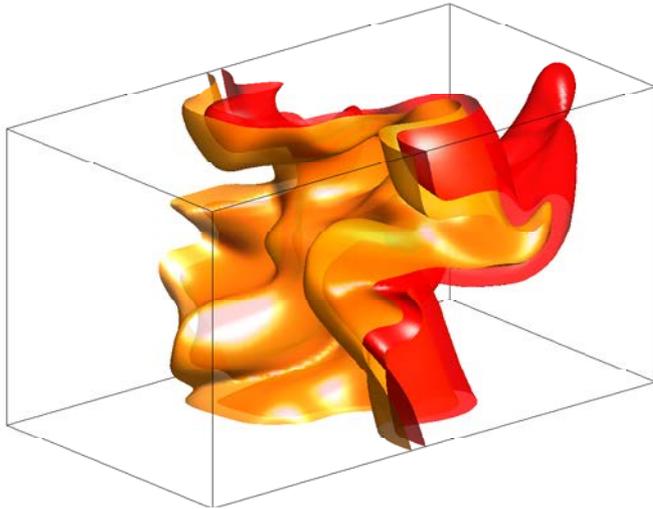
Turbulent Inflow / Outflow
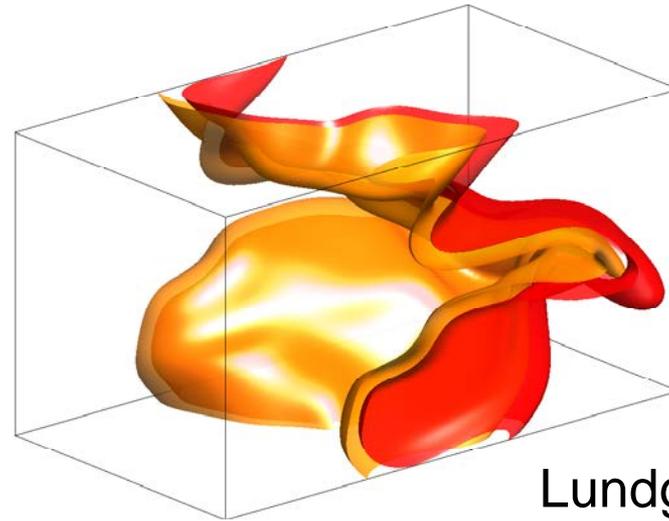
Lundgren Forcing
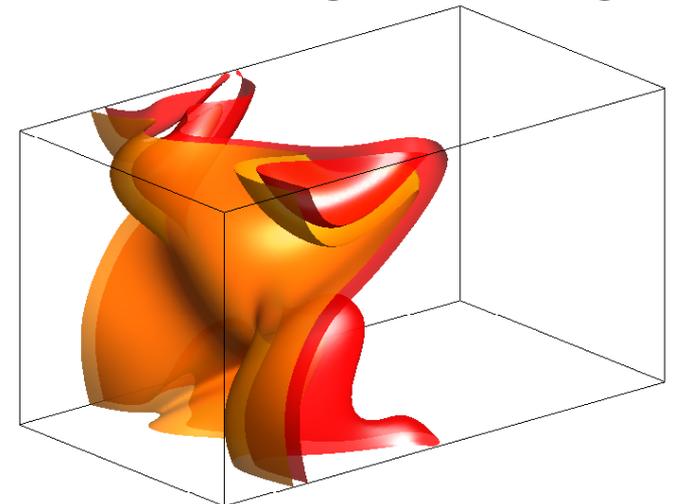
Instantaneous view of c isosurfaces.
The value of c increases from 0.1 to 0.9
from yellow to red. From left to right:

DT / IO / LF

Decaying turbulence

- The energy spectrum can <u>only</u> be prescribed at start of simulation

- By the time statistics were extracted u'/S_L in the unburned gas decayed by about 50% whereas l/δ_{th} increased by about 1.7 times

- This indicates Re_t decreased by roughly 15%.

- There is a history effect

- Run time is short, typically 2-4 eddy turnover times $t_e = l/u'$

- Data is typically (but not necessarily) taken from a single frame where TKE and global burning rate were not changing rapidly

Inflow / Outflow configuration

- Temporal decay of energy in the DT is now a spatial decay

- Spatial decay of TKE comes along with an increase of length scales

- The point of flame stabilization is not known *a-priori* and consequently turbulence parameters cannot be controlled

- As the flame moves back and forth the turbulence parameters change and consequently there is a history effect as well.

- A long axial domain size is required. If the flame is initially located at its centre, turbulence likely has decayed considerably.
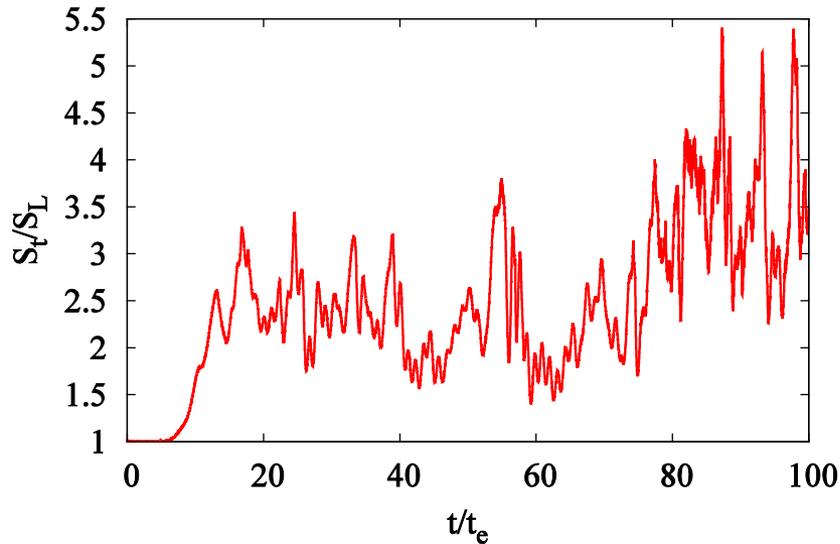
Variation of turbulent flame speed over time for an IO configuration.
Inflow velocity is a filtered version of S_T.

- Under conditions of low u'/S_L and large l, it is possible to obtain an instability of combined action of Landau-Darrieu / thermo-diffusive type or of Rayleigh Taylor type, introduced by a variable inflow rate.

- It is nearly impossible to obtain a long term steady state simulation of $u'/S_L > 3$

- A long domain is needed combined with run times $\gg 50 t_e$.

Lundgren Forcing method

- TKE and l can be maintained spatially and temporally

- However, l cannot be controlled and converges to 35% domain size.

- As a consequence Da and Ka cannot be properly adjusted

- This can be explained as follows. For a Kolmogorov Spectrum:

$$k = \int_{2\pi/\text{L}}^{\pi/\Delta} E(\kappa)\, d\kappa \approx C_k \varepsilon^{\frac{2}{3}} \frac{3}{2} \left(\frac{2\pi}{L}\right)^{-\frac{2}{3}} \Rightarrow \frac{k^{\frac{3}{2}}}{\varepsilon} \approx \frac{\left(C_k \frac{3}{2}\right)^{\frac{3}{2}}}{2\pi} L \Rightarrow l \approx 0.54L$$

(a bit too large) where L is the domain size and Δ the filter width.
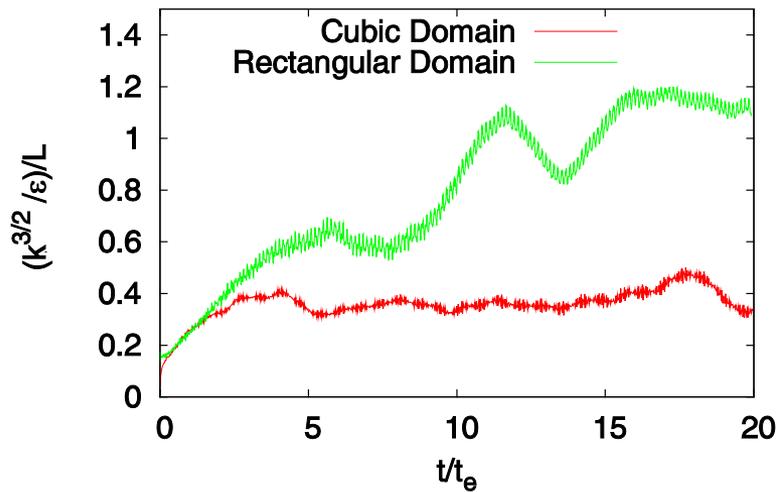
Development of the normalized length scale $(k^{\frac{3}{2}}/\varepsilon)/L$ with non-dimensional time t/t_e in a cubic domain and a rectangular domain, for an isothermal Lundgren-forced flow.

- There are problems with rectangular domains.

- If applied globally, the forcing tries to enforce a constant level of turbulence and length scales on both sides of the flame.

- LF method requires a rather long run time before a statistically steady state is achieved and also a large domain.

- Forcing can be applied on the unburned gas side but this requires some modifications.

An evolution equation for l can be derived by taking the logarithm of $l = k^{\frac{3}{2}}/\varepsilon$ which gives $\ln(l) = 3/2\ln(k) - \ln(\varepsilon)$ and by differentiation

$$\frac{1}{l}\frac{Dl}{Dt} = \frac{3}{2}\frac{1}{k}\frac{Dk}{Dt} - \frac{1}{\varepsilon}\frac{D\varepsilon}{Dt}$$

TKE reaches its steady state relatively fast in the LF forcing.
It takes considerably longer until l reaches its asymptotic limit.

During this state (i.e. $Dk/Dt = 0$) and for homogeneous, incompressible turbulence the eqn. can be simplified using the exact ε transp.equation:

$$\frac{Dl}{Dt} = \frac{l}{\varepsilon}\left[2\overline{\left(\nu\frac{\partial^2 u_i}{\partial x_k \partial x_m} \right)^2} - \frac{\varepsilon^2}{k} - 2\nu\overline{\frac{\partial u_i}{\partial x_m}\frac{\partial u_k}{\partial x_m}\frac{\partial u_i}{\partial x_k}} \right]$$

T_D: dissipation T_F:forcing T_P:turb. prod.

It will be interesting to understand how these terms behave.

- For a steady state we have $T_D - T_F - T_P = 0$.

- In the modelled ε transport equation $T_P = 0, T_D = C_{\varepsilon 2}\dfrac{\varepsilon^2}{k} = C_{\varepsilon 2}\,T_F$

- This lead researchers to the conclusion that $C_{\varepsilon 2} = 1$ which isn't true.

- If T_P is modelled as $\overline{2\nu\dfrac{\partial u_i}{\partial x_m}\dfrac{\partial u_k}{\partial x_m}\dfrac{\partial u_i}{\partial x_k}} \sim 2\nu\left(\dfrac{u'}{\lambda}\right)^3$ the resulting eqn. Is

$$\frac{Dl}{Dt} = k^{1/2}\left[C_{\varepsilon 2} - 1 - C_P\sqrt{Re_l}\right] \quad Re_l = \frac{k^{1/2}\,l}{\nu}$$

- This has the problem that l would be dependent on viscosity

- From analysis of DNS data it turns out that in fact:

  - $T_P > T_F$

  - The scaling $T_P = \overline{2\nu\dfrac{\partial u_i}{\partial x_m}\dfrac{\partial u_k}{\partial x_m}\dfrac{\partial u_i}{\partial x_k}} \sim 2\nu\left(\dfrac{u'}{\lambda}\right)^3$ is correct !

  - Hence, $T_D = C_D\dfrac{\varepsilon^2}{k}, \quad C_D = C_D(Re_l)$ which is indeed observed.

Idea to circumvent some problems of LF − filtered forcing:

$$f = \max[0, (k_{target} - k)/(\Delta t k_{target})] \; \bar{u}^{HP} \;\; \text{where} \;\; \bar{u}^{HP} = u - \bar{u}$$
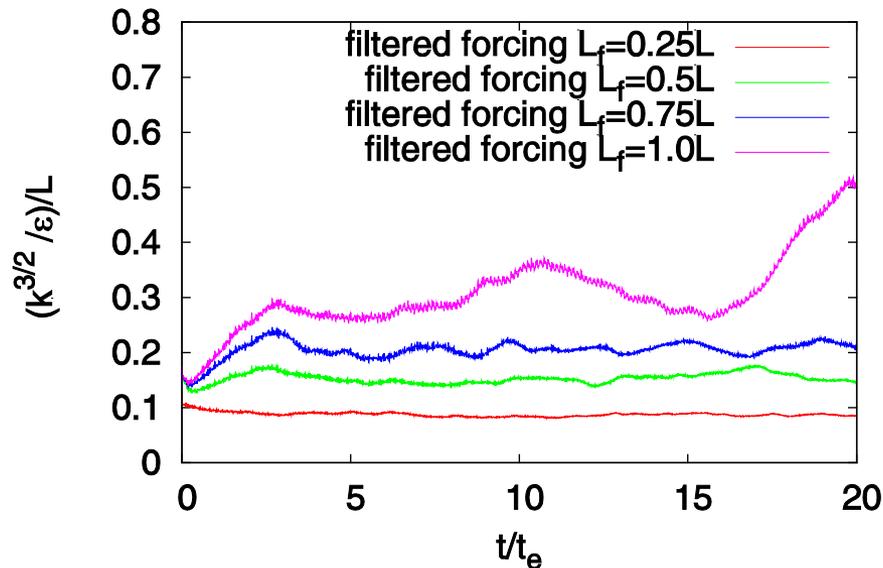
Development of the normalized length scale $(k^{\frac{3}{2}}/\varepsilon)/L$ with non-dimensional time t/t_e in a cubic domain and a rectangular domain, for an isothermal Lundgren-forced flow.
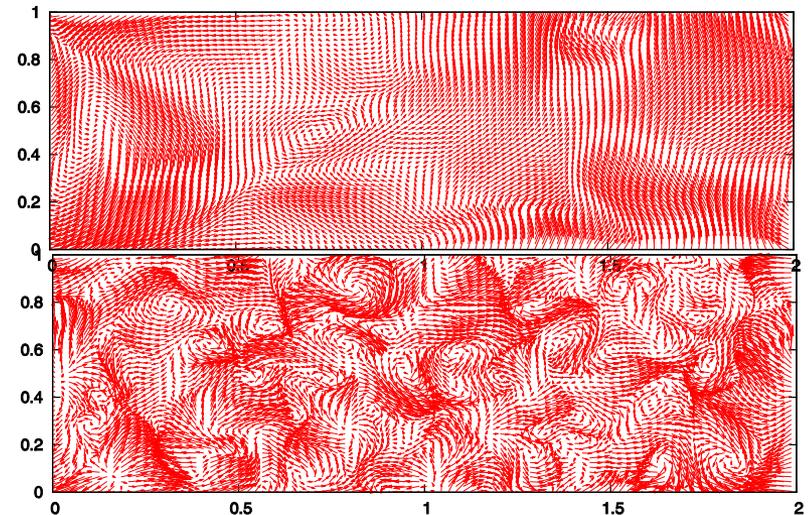
Instantaneous velocity field in a rectangular domain with a high pass filtered forcing term of characteristic length $L_f = L$ (top) $L_f = L/4$ (bottom).

Results from band with limited forcing
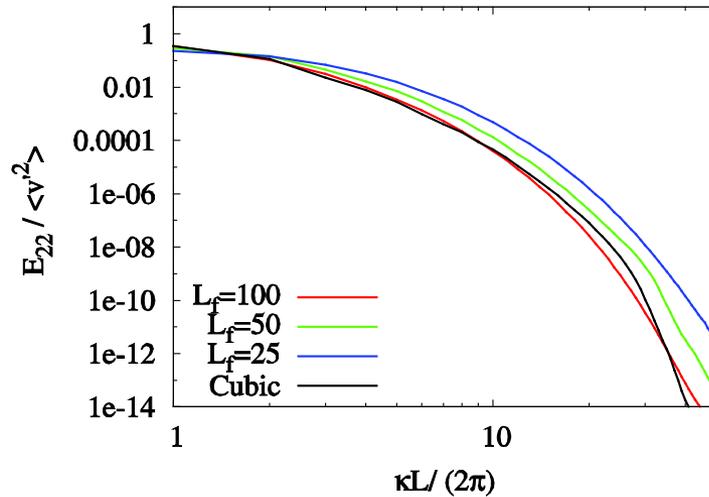
One dimensional energy spectra using the filtered forcing method in comparison to the unfiltered forcing in a cubic domain.
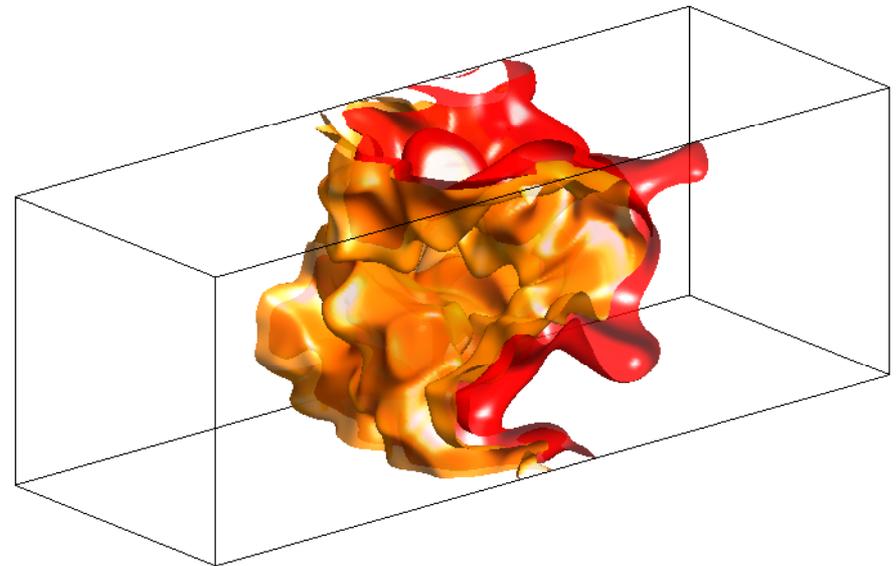
Planar flame with filtered forcing applied to the unburned gas side only.

Conclusions

- The gradient flux resp. Eddy viscosity assumptions give very bad predictions within the flame brush even for the highest Reynolds numbers considered.

- Scale Similarity Models perform considerably better. However, it is important to better understand how they are influenced by numerical errors.

- There is potential for model improvement in combustion LES and a-priori analysis is in my opinion a useful tool to drive this and to understand the interaction between physics and numerics.

- Dynamic evaluation of model parameters can be quite difficult within the flame brush. Model parameters are essentially a function of reaction progress.

- All findings remained qualitatively unchanged for higher Reynolds number and for detailed chemistry !

- The Yoshizawa model for estimating GSGS TKE considerably underpredicts for large filter size. It should <u>not</u> be used for LES quality assessment !

- Three methods to simulate planar flames have been compared. All methods have considerable disadvantages. To me the simplest method (DT) is not really worse than the others.

- The Lundgren Forcing method is an appealing idea but in my opinion some refinements are required.

- A proposal has been made how some disadvantages of LF can be avoided.

Thank your for your attention !